A Physics Study for Reflector Temperature Coefficient (RTC) of Small Molten Salt Fast Reactor (MSFR)

Young-June Lee, Eunhyug Lee, and Yonghee Kim*
Department of Nuclear & Quantum Engineering, Korea Advanced Institute of Science and Technology (KAIST), 291 Daehak-ro, Yuseong-gu, Daejeon 34141, Republic of Korea
**Corresponding author: yongheekim@kaist.ac.kr*

Keywords: Molten Salt Reactor (MSR), Reflector Temperature Coefficient (RTC), Local Spectrum Hardening

1. Introduction

Among the advanced GEN IV reactors, Molten Salt Reactor (MSR) has been in the limelight as an optimum design for micro or maritime application of nuclear technology: Fuel salt acts as both nuclear fuel and coolant in the primary loop, which render extremely simple system. Furthermore, its superior inherent safety is guaranteed by the strongly negative fuel temperature coefficient which emanates from the distinctive feature of MSR, the dimensional expansion of nuclear fuel itself.

Driven by the demand to secure the targeted operational lifespan without refueling and minimize the loading of 19.75 % HAELU (High-Assay Low-Enriched Uranium), the light nuclei-based reflector should be involved. Furthermore, the usage of reflector is inevitable in terms of securing shielding, safety features and simple reactivity control mechanism stemming from the surgical moderation effect in the periphery of the active core.

Despite the overall advantages of the reflector in terms of neutronics, the loading of reflector should be marginal: Over-loaded reflector may cause the positive Reflector Temperature Coefficient (RTC) which deteriorates the inherent safety. Unlike the LWR, which is utilizing liquid moderator, light water, the solid reflector always causes the positive RTC in the over-moderated sense. Consequently, a physics study for RTC of small Molten Salt Fast Reactor (MSFR) has been conducted to reveal the underlying mechanism for the positive RTC and investigate the suitability of various reflector material for MSR, such as Beryllium (Be), Beryllium Oxide (BeO), Graphite and Magnesium Oxide (MgO).

2. Analysis Model for RTC of MSFR

The active core is a simple cylindrical geometry with same diameter and height of 160 cm, where it is surrounded by the SS316 barrier of 0.8 cm and Inconel 625 cladding of 0.08 cm. In the outermost side, 2.5 cm SS304 vessel surrounds the reflector region.

For the fuel salt, NaCl-KCl-UCl_3 ternary salt has been utilized. Molar composition of NaCl-KCl-UCl_3 is 42.9-20.3-36.8 with 19.75 wt.% HALEU, which corresponds to the lowest eutectic temperature, 470.15 ℃. To minimize the parasitic neutron absorption by chlorine, 99 wt.% Cl-37 has been utilized. The temperature of fuel salt is fixed at 900 K which corresponds to the density of 3.3933 g/cm^3.

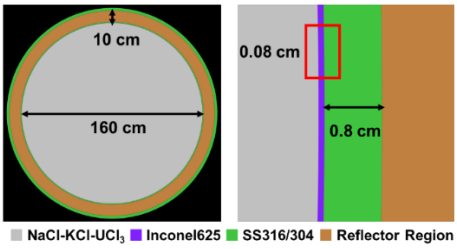

Fig 1. Side view of MSFR

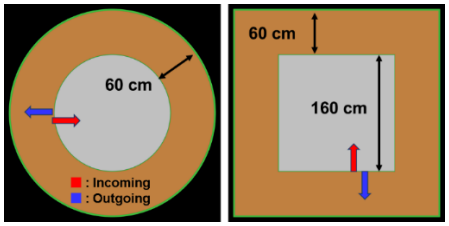

Fig 2. Side and Top view of MSFR

For the relfector material, Beryllium (Be), Beryllium Oxide (BeO), Graphite and Magnesium Oxide (MgO) have been utilized with simultaneously varying the radial and axial thickness from 10 cm to 60 cm as shown in Figs. 1 and 2. TABLE I enumerates the density of reflector materials. For BeO and MgO, 99 % TD have been used.

TABLE I. Density of Reflector Materials

Material	Be	BeO	Graphite	MgO
g/cm^3	1.848	2.9799	1.70	3.5442

Assuming the isothermal temperature of 900 K in the nominal state, the neutron multiplication factor has been evaluated by varying the thickness of various reflector materials. Monte Carlo-based criticality calculation code, Serpent 2.2.1 and ENDF/B-VII.1 library have been used with 200,000 histories per cycle, 100 inactive and 300 active cycle, which lead to the uncertainty of 9 pcm regarding the k_{eff}. S (α, β) thermal scattering law has been applied to Be, BeO and Graphite.

Starting from the k_{eff} without any reflector, which corresponds to 0.65148, it gradually becomes saturated in the vicinity of 60 cm thickness as shown in Fig. 3. Among them, BeO is the most favorable material to secure the excess reactivity due to its high moderating ratio and (n, 2n) reaction of Be-9.

Fig. 4 depicts the calculated RTC corresponding to Fig. 3, by varying the temperature from 900 K to 1000 K

excluding the fuel salt. Thermal scattering law (TSL) also has been applied for varying temperature. As shown in Fig. 4, despite the similar reactivity worth between Be and BeO, the RTC of Be is clearly more positive.

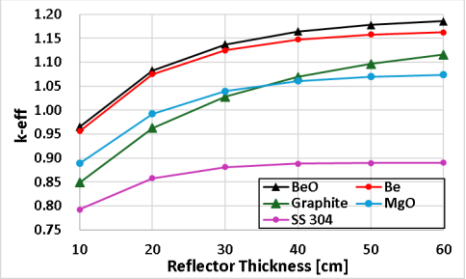

Fig 3. k_{eff} profile of each reflector materials

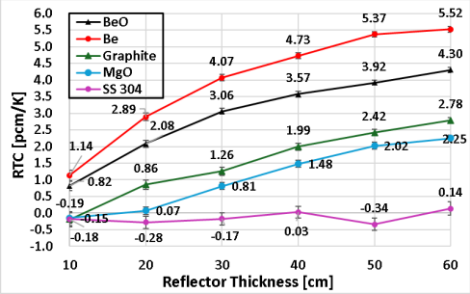

Fig 4. RTC profile of four reflector materials

3. Numerical Results

3.1 Underlying Physics of Positive RTC in MSFR

To figure out the reason that RTC becomes positive in MSFR, the case of BeO reflector with 18.8 cm thickness has been adopted. Neutron spectrum, flux, current at the surface of the active core and major reaction rates have been tallied. For the evaluation, 500,000 histories per cycle, 100 inactive and 300 active cycle have been used.

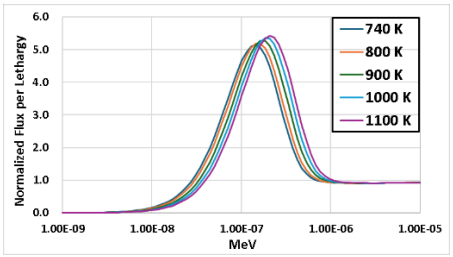

Fig 5. Reflector Spectrum in thermal energy region

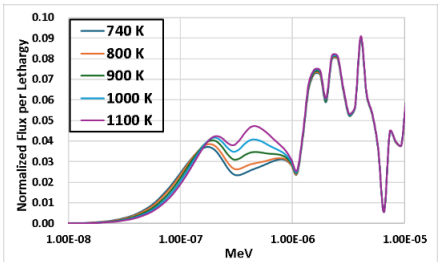

Fig 6. Active Core Spectrum in thermal energy region

As shown in Fig. 5, when the temperature of reflector material increases, local spectrum hardening happens in thermal energy region, especially in the vicinity of the thermal peak. This is because the energy where neutrons reach in thermal equilibrium sate with its media becomes increases in an inelastic way due to the excitation of reflector atoms or increased phonon density in the lattice structure. This results in the local spectrum hardening.

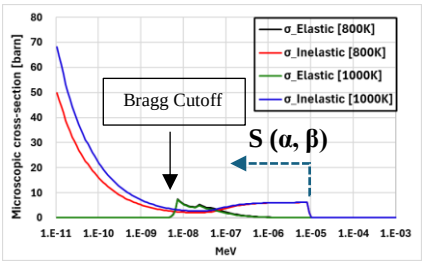

Fig 7. TSL applied cross-section of Beryllium (Be)

To figure out above phenomena in a physical way, TSL applied scattering XS need to be considered. Fig. 7 shows the elastic (coherent) and inelastic (incoherent) scattering XS of Be in two different temperatures. Below the Bragg cutoff energy, the coherent elastic (Bragg) scattering cannot happen since the Bragg reflection of neutron is forbidden. Bragg cutoff energy itself depends on the crystal structure of material. In case of BeO, since the maximum inter-planar distance is d_{100} = 2.366 Å, neutrons which wave-length $\lambda > 2d_{100}$ = 4.672 Å (E < 3.76 meV) cannot experience the Bragg scattering [1]. It can be also observed in Fig 9.

After the Bragg cutoff energy, the coherent elastic scattering discontinuously increases and becomes smoother due to contributions of neutron reflection from many Bragg planes which satisfy the condition $n\lambda=2d_{hkl}\sin\theta$. As the coherent elastic scattering decreases proportionally to increasing neutron energy, the inelastic scattering gradually increases since the tendency of scattering phenomena itself cannot disappear suddenly. Since the scattering phenomena after the Bragg cutoff energy is closely related to quantized phenomena, the scattering XS hardly changes in this energy region although the temperature increases or decreases.

However, below the Bragg cutoff energy, there is a significant increase of inelastic scattering as the temperature increases, which allows the up-scattering of neutron, due to the thermal motion of excited reflector atoms and increased phonon density. This is the root-cause of local spectrum hardening.

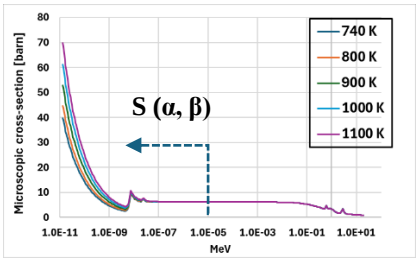

Fig 8. Total scattering cross-section of Be

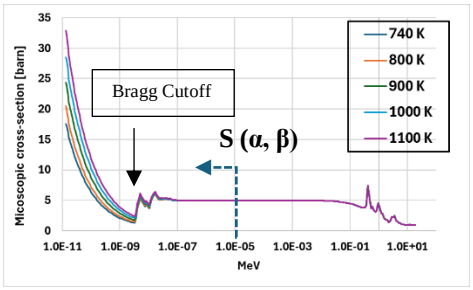

Fig 9. Effective Total scattering cross-section of BeO

However, since it is a marginal effect near the thermal peak, the decrement of parasitic absorption of thermal neutron by reflector and other materials, such as SS and Inconel625, overwhelms the decrement of moderation effect in the over-moderated sense. This means that more thermal neutrons can re-enter the active core by escaping from the parasitic absorption.

Resultantly, the local spectrum softening happens in the active core as shown in Fig. 6, which is the root-cause of positive RTC. In this sense, it is crystal-clear that the RTC of SS reflector should be nearly zero as shown in Fig. 4. Noteworthy is that all the following results are normalized based on the fixed fission power of $100MW_{th}$.

TABLE II. Effective Microscopic capture XS of BeO
(Unit: barn · 1E-3)

[Kelvin]	740	800	900	1000	1100
Total	1.79	1.75	1.71	1.67	1.63
Thermal	2.60	2.52	2.39	2.29	2.20
Fast	1.273	1.273	1.272	1.272	1.271

Effective microscopic capture cross-section of BeO has been evaluated as given in Eq. (1). Capture means all the neutron disappearance reactions which do not produce secondary neutron, such as radiative capture, (n, α) reaction, etc. Thermal indicates the energy range up to 1 eV and fast indicates the energy range from 1 eV to 20 MeV.

$$\tilde{\sigma}_x = \frac{\int (\sigma_{x1}(E) * N_1 + \sigma_{x2}(E) * N_2) * \phi(E,r)\, dEdr}{N * \int \phi(E,r)\, dEdr} \quad (1)$$

As shown in TABLE II, the effective microscopic capture cross-section of BeO decreases in higher temperature. Particularly, the decrement is dominant in thermal energy region due to the local spectrum hardening.

TABLE III. Neutron Current at 900 K

900 K	**Thermal**	**Fast**	**Total**
Net Current	7.45E+17	2.75E+18	2.00E+18
Outgoing	8.08E+16	1.18E+19	1.19E+19
Incoming	8.26E+17	9.04E+18	9.86E+18

TABLE IV. Variation of Thermal Neutron Current

Thermal	**740 K**	**800 K**	**1000 K**	**1100 K**
Net	1.4E+16	8.2E+15	6.3E+15	1.2E+16
Out	5.8E+15	3.7E+15	3.6E+15	7.0E+15
In	1.9E+16	1.2E+16	9.9E+15	1.9E+16

TABLE V. Variation of Fast Neutron Current

Fast	**740 K**	**800 K**	**1000 K**	**1100 K**
Net	1.0E+16	6.3E+15	5.6E+15	1.2E+16
Out	3.8E+16	2.2E+16	1.9E+16	4.1E+16
In	2.7E+16	1.6E+16	1.4E+16	2.9E+16

TABLE III enumerates the surface-weighted neutron current on the surface of the active core at nominal state, 900K. The outgoing and incoming directions are depicted in Fig. 2. Red color indicates negative value. The variations in this paper including the TABLE IV and V are calculated based on the nominal state as given in Eq. (2) and the net current is estimated as given in Eq. (3).

$$Q(740\ K\ \ldots\ 1100\ K) - Q(900\ K) \quad (2)$$

$$Net\ Current = Incoming - Outgoing \quad (3)$$

As shown in TABLE IV, as the temperature becomes higher, the incoming partial current of thermal neutrons increases due to the re-entering effect. Consequently, the net current of thermal neutrons increases in the way of incoming direction which also accord with the spectrum softening of the active core. This means that the active core region becomes more fission-friendly environment.

Furthermore, variations of other physical quantities such as leakage rate, microscopic fission and capture cross section in the fuel salt, release energy or neutrons per fission and (n, Xn) reactions all accord with the local spectrum shift in the MSFR as the reflector region temperature increases.

TABLE VI enumerates the k_{eff} of serpent results and reproduced k_{eff} by using tallied reaction rates as given in Eq. (4). The discrepancy about 1 – 2 pcm is due to the minor (n, Xn) reaction rate such as SS and Inconel625.

$$k_{eff} = \frac{\nu * R_f}{R_c + R_f - R_{(n,2n)} - 2 * R_{(n,3n)} - 3 * R_{(n,4n)} + R_{Leakage}} \quad (4)$$

TABLE VI. k_{eff} Reproduced by R.R vs. Serpent Results

[Kelvin]	**740**	**800**	**900**	**1000**	**1100**
Reproduced	1.06767	1.06920	1.07156	1.07353	1.07569
Serpent Results	1.06768	1.06922	1.07158	1.07355	1.07571
RTC	2.40	2.20	1.84	2.01	-

TABLE VII. Variation of major reaction rates [unit: #/s]

[Kelvin]	**740**	**800**	**1000**	**1100**
Capture (Reflector)	4.5E+16	2.7E+16	2.4E+16	4.7E+16
Capture (Fuel)	3.0E+15	1.9E+15	1.6E+15	3.6E+15
ν * Σ(f)	5.8E+14	3.8E+14	2.7E+14	5.0E+14
Leakage	2.1E+16	1.3E+16	1.2E+16	2.3E+16

TABLE VII enumerates the variation of major reaction rates. Since the reaction rates are normalized based on the

fission power rate, main changes only occur in the capture reaction rate of the reflector region and the leakage rate. These two quantities are the main indicators that represent the easiness or difficultness of fission reaction in the active core. However, the variation of (n, xn) reaction rates are negligible, so it hardly affects the RTC unlike the FTC.

3.2 Comparison of RTC with different reflectors

To compare the RTC of different reflector materials, the thickness of each materials has been adjusted as shown in TABLE VIII, to secure similar excess reactivity each other. Fig. 10 depicts the normalized whole core spectrum for the four cases.

TABLE VIII. Reflector thickness and k_{eff} of four cases

Material	BeO	Be	Graphite	MgO
k_{eff}	1.07172	1.07177	1.07163	1.07162
[cm]	18.8	20	41.5	60

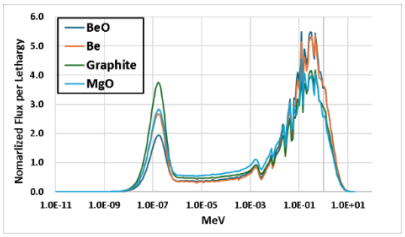

Fig 10. Normalized Spectrum for four materials

Similar to the case of BeO, the same local spectrum shift happened in Be, Graphite and MgO cases. Also, the variation of neutron spectrum, flux, current at the surface of the active core and major reaction rates showed same trend with BeO reflector.

TABLE IX. Variation of major reaction rates [Be]

[Kelvin]	**740**	**800**	**1000**	**1100**
Capture (Reflector)	6.3E+16	3.8E+16	3.3E+16	6.3E+16
Capture (Fuel)	4.6E+15	2.9E+15	2.6E+15	4.7E+15
$\nu * \Sigma(f)$	7.7E+14	4.7E+14	4.1E+14	7.2E+14
Leakage	2.7E+16	1.6E+16	1.4E+16	2.8E+16

TABLE X. Variation of major reaction rates [Graphite]

[Kelvin]	**740**	**800**	**1000**	**1100**
Capture (Reflector)	5.3E+16	3.2E+16	2.8E+16	5.4E+16
Capture (Fuel)	3.3E+15	2.2E+15	2.0E+15	3.8E+15
$\nu * \Sigma(f)$	6.1E+14	3.7E+14	3.0E+14	5.4E+14
Leakage	2.7E+16	1.7E+16	1.4E+16	2.8E+16

TABLE XI. Variation of major reaction rates [MgO]

[Kelvin]	**740**	**800**	**1000**	**1100**
Capture (Reflector)	4.2E+16	2.6E+16	2.2E+16	4.3E+16
Capture (Fuel)	5.4E+15	3.1E+15	2.9E+15	5.5E+15
$\nu * \Sigma(f)$	7.2E+14	4.3E+14	3.6E+14	7.3E+14
Leakage	1.7E+16	1.0E+16	1.0E+16	1.9E+16

TABLE XIII enumerates the calculated RTC [pcm/K] of four different materials. The uncertainty of RTC is about 0.07 [pcm/K]. TABLE XII shows the effective total scattering XS of BeO, Be and Graphite in the energy range below the Bragg cutoff, 1E-8 MeV, where the inelastic scattering is dominant. As the temperature increases, the scattering XS increase due to the clearly enhanced inelastic scattering also as shown in Figs 8 and 9.

Among three materials, Be has clearly largest effective inelastic scattering XS, where it leads to the significant up-scattering of neutrons and most positive RTC. By contrast, the inelastic scattering XS of BeO is slightly lower than that of Graphite, where it results in slightly less positive RTC.

In case of MgO, there is no available S (α, β) library in ENDF/B-VII.1. Although evaluated RTC is somewhat similar whether the TSL is applied or not, since it is not a pure thermal reactor, the RTC of MgO needs to be evaluated with TSL in a refined and physical way.

TABLE XII. Effective Total Scattering XS [unit: barn]

[Kelvin]	740	800	900	1000	1100
BeO	3.84	3.96	4.17	4.39	4.60
Be	6.43	6.64	7.00	7.36	7.71
Graphite	4.67	4.76	4.91	5.07	5.23

TABLE XIII. RTC of four different reflector materials

[Kelvin]	**740-800**	**800-900**	**900-1000**	**1000-1100**
BeO	2.40	2.20	1.84	2.01
Be	3.61	3.31	2.80	2.58
Graphite	2.65	2.37	2.16	1.91
MgO	2.62	2.53	2.04	1.97

4. Conclusion

The underlying physics of Reflector Temperature Coefficient (RTC) of Molten Salt Fast Reactor (MSFR) has been investigated. The RTC of BeO has been evaluated clearly less positive than the metallic Be. This reveals the advantage of oxide material in terms of RTC.

ACKNOWLEDGEMENT

This research was supported by Korea Atomic Energy Research Institute (NTIS-1711199027), grant funded by the Korean Government (MSIT) (RS-2023-00260898) and Korea Research Institute for defense Technology planning and advancement (KRIT) grant funded by the Korea government (DAPA (Defense Acquisition Program Administration)) (KRIT-CT-22-017, Next Generation Multi-Purpose High Power Generation Technology (Liquid Fueled Heat Supply Module Design Technology), 2022).

REFERENCES

[1] Al-Qasir, Iyad, et al. "Thermal neutron scattering cross sections of beryllium and magnesium oxides." *Annals of Nuclear Energy* 87 (2016): 242-251.